Materials Research. 2017; 20(2): 532-537
DOI: http://dx.doi.org/10.1590/1980-5373-MR-2016-0603

Electrical Conductivity in the KDP, ADP, and $K_{1-x}(NH_4)_xH_2PO_4$ Crystals

Fabrício Mendes Souza*[a]

[a] *Universidade do Estado de Minas Gerais, 3001, Paraná Avenue, Divinópolis, 35501170, MG, Brazil*

Received: August 17, 2016; Revised: January 03, 2017; Accepted: February 02, 2017

Impedance Spectroscopy was performed to examine the electrical conductivity on KH_2PO_4 KDP, $(NH_4)H_2PO_4$ ADP and $K_{1-x}(NH_4)_xH_2PO_4$ ($x = 0.076, 0.118, 0.357, 0.857, 0.942$) crystals with increasing temperature. They were grown by solvent evaporation method. Zview simulation software was used to theoretically fit electrical conductivity results as a function of frequency (1-10^6 Hz) and temperature (20-160 ºC) with equivalent circuits. These dielectric-type materials become ionic conductors upon heating. Proton jumps in hydrogen bonds, heavier ions migration (K^+ and NH_4^+), and rotation and reorientation of ammonium groups contributed to electrical conduction. This conduction behavior follows the Arrhenius equation with which the activation energies were determined at different temperature ranges. For ADP-rich ($x > 0.8$) and pure ADP crystals the conductivities are higher than those for KDP-rich ($x < 0.2$) and pure KDP. Lattice defects may reduce electrical conductivities in the crystals with intermediate x composition. Complex permittivity ac and complex conductivity *ac* were also obtained for these crystals.

Keywords: *mixed crystals, KDP, ADP, electrical conductivity, non-linear optical materials, Impedance Spectroscopy, crystalline defects*

1. Introduction

Crystals of ammonium dihydrogen and potassium dihydrogen phosphates, $NH_4H_2PO_4$ (ADP) and KH_2PO_4 (KDP), as well as $K_{1-x}(NH_4)_xH_2PO_4$ ($KADP_x$) have been extensively studied, owing to their potential applications in electro-optical units. The areas of laser radiation non-linear transformers and ferroelectricity motivate the examination of these crystals[1-4]. KDP and ADP crystallize in the tetragonal system with the same space group. The crystal growth can be performed by spontaneous nucleation in aqueous solution, in which the competition between NH_4^+ and K^+ with the $H_2PO_4^-$ groups occurs during the ionic bonding[5,6]. This competition leads to the unit cell expansion in the $KADP_x$ crystals, owing to the ammonium entrance in a relatively K^+ small room. Thus, the local areas of the crystal frame expand to accept the larger cations (NH_4^+)[6]. As a result, structural stress, distortions of crystal lattice, cracks and defects within the mixed crystal frame can occur, causing damage in the crystal quality[3,7]. These microstructural aspects are related to the HN-O and K-O bond strengths, as well as, to the differences of the size of the cationic radius - NH_4^+ ion (ionic radius 1.42Å) or K^+ ion (ionic radius 1.33Å) in the mixed crystals. Moreover, there are different amounts of these cations in each mixed crystal and it is known that distances between (100), (101), (001), (110), and (112) crystalline planes in the ADP crystal are greater than those in the KDP crystal[7]. When KDP is heated at higher temperatures, there is a loss of H_2O molecules and the formation of phosphoric acid. On the other hand, ADP lose mass with ammonia formation[8,9]. The differences in the bond strength lead to the intrinsic detachment behaviors of the molecules in each crystal frame, conducting to their decomposition[6].

Impedance spectroscopy is largely used in the characterization of the electrical properties of different materials (ordered or disordered solids), dielectrics for instance. This technique permits the determination of the electric and dielectric properties of a specific material, as well as, correlates them with the micro-structural defects, in general, in a frequency range, f, between 10^{-4} and 10^7 Hz. The study of the dependence between electrical conductivity and signal frequency applied to the material can be done through the dielectric behavior results by using dielectric permittivity ε^* as a function of the frequency ($\omega = 2\pi f$), or using the ionic conductor behavior, that expresses the electrical conductivity results, $\sigma^*(\omega)$, which can be expounded as complex impedance results, $Z^*(\omega)$[10,11].

In this work, *ac* impedance and *dc* impedance were used to characterize the electrical conductivity of the crystals as a function of the frequency and as a function of the temperature for the 20 ºC - 160 ºC temperature range. The study of the conductivity dependency with composition x, as well as, with temperature, was done through the analysis of the complex impedance data, which has been written in the superposition of the two Cole-Cole expressions that represent the proposed microscopic conduction of the crystals. This relation correlates physical phenomenon to the theoretical data with equivalent circuits as two R−C parallel in series[11].

* e-mail: souzafm@yahoo.com.br

2. Materials and methods

The KDP (x = 0), ADP (x = 1.0), and $KADP_x$ hybrid crystals (x = 0.076, 0.118, 0.357, 0.857 and 0.942) were grown by evaporation at 40°C from the aqueous solution. Pure deionized water of 18.2 MΩcm was used as the solvent. Crystals were prepared as little plate shapes in the [100] direction with application of silver ink (electrodes) on the greater surfaces (superior and inferior)[6]. The electrical measurements were carried out in the temperature range of 20 ºC - 160 ºC under vacuum. The complex impedance (Z*) was determined in the frequency range from 1 Hz to 10^6 Hz with an applied potential of 2 V using an impedance analyzer Solartron (SI 1260). The molar percentages of x for the mixed crystals were determined by obtaining the potassium amount with Inductively Coupled Plasma - Atomic Emission Spectrometry *ICP-AES* technique by using a Spectro (Ciros CCD) spectrometer. The potassium element amount was obtained in duplicate by using the wave length from the potassium detection. The ammonium amount was obtained by the diminution 1 - x, for the different crystals. Hence, $KADP_x$ mixed crystals were grown with the molar quantities[6] x = 0.076, 0.118, 0.357, 0.857, and 0.942. The experiments were performed at *Universidade Federal de Ouro Preto (UFOP)*, MG, Brazil.

3. Results and Discussion

External electric field action can induce a polarization in the material, and consequently, an electrical current emerges through the charge conduction. An electrical current appears in the material under an alternate electric field with frequency variation, which induces to a phase angle between the applied voltage and the electric current. Besides, another out of phase component related to frequency and time delay of electric dipoles relaxation also appears[10,11]. Pure KDP and ADP crystals are dielectrics (non electric conductors) at low temperatures and gradually become ionic conductors as the temperature is increased. Accordingly, physical polarization processes and ionic conduction occur when crystals are heated. Conduction mechanisms have been observed in these crystals and they happen due to the hopping effect during the protons migration across hydrogen ions vacancies in the crystalline lattice[6,8,9]. Some authors reported about three types of defects, which, in this case, lead to the electric conduction that involves the movement or jump of hydrogen ions between the constituent's bonds in the crystal bulk. Furthermore, the movement of hydrogen, potassium, and ammonium ions contribute to the increase in the electrical conductivity at higher temperature[8,9,12,13].

The electrical conductivity results are shown by complex impedance $Z^*(\omega)$ of the KDP, ADP, and mixed crystals in Figure 1. This figure shows the graphics of the real impedance (Z') and imaginary impedance (Z'') as a function of frequency (with a double log scale) for the 20 ºC - 160 ºC temperature range. The frequency of the relaxation peaks can be interpreted as two parts one involving the bulk of the samples, which is the rapid relaxation mechanisms (at higher frequencies), and another one involving the surface effect of electrode, which represents the slow relaxation mechanisms (at lower frequencies). Thus, the complex impedance can be written by two superposition expressions[10,11]:

$$Z^*(\omega) = \frac{1/G_1}{1+(i\omega\tau_1)^{1-m}} + \frac{1/G_2}{1+(i\omega\tau_2)^{1-n}} \text{ where } \tau_1 = \frac{1}{\omega_{p1}} = \frac{C_1}{G_1}\ \tau_2 = \frac{1}{\omega_{p2}} = \frac{C_2}{G_2} \quad (1)$$

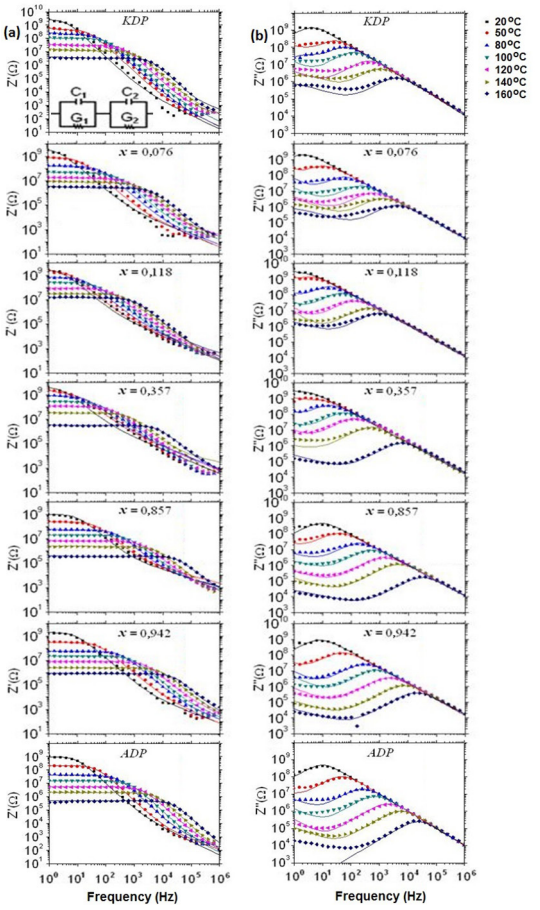

Figure 1: Electrical conductivity, as a function of frequency (with a double log scale) on the 20 ºC - 160 ºC temperature range, represented by complex impedance $Z^*(\omega)$, real impedance (Z') and imaginary impedance (Z''), for the KDP, ADP, and mixed crystals.

where the ω_{p1} and ω_{p2} are the intrinsic angular frequencies of the maximum points on the Z'' curves and τ_1 and τ_2 the respective relaxation times. The fitting of the real impedance (Z') and imaginary impedance (Z'') was done by using a simulation software (Zview). The parameters m and n are entrance data which complements the Z' and Z'' fitting at higher and lower frequencies. Figure 1 presents the equivalent circuit used to represent electrical conduction mechanisms in the crystals in order to describe the electrical

conduction behavior of the crystals. This equivalent circuit of two R−C parallel circuits in series (Figure 1), one G_1−C_1 parallel represents the bulk and another one G_2−C_2 parallel represents the surface effect of the electrode on the crystals.

The electrode surface effect fitting at low frequencies on the ADP in the Z'' in 160 ºC was not reached, owing to the *Zview* simulation limiting value. The conductivity of all crystals increases with increasing temperature. Hence, the real impedance curves decreases at higher frequencies and at higher temperatures. Thus, the impedance results of the mixed crystals are close to the impedance results of pure crystals (Figure 1). The solid lines represent the theoretical fits (Eq. 1) obtained by the use of the RC circuit simulation, which represents the physical behavior of the experimental results, Figure 1.

Figure 1 shows Z' curves which have a tiny dependency with the frequency in the *ac* conductivities on the crystals at low frequency regions, but at high frequencies, the conductivities increase to higher frequencies with a gradual changing as the temperature is increased (diminutions on the Z' curves - 'knees') on both curves (Z' and Z''). The shifts of the 'knees' on the Z' curves change to higher frequencies as the temperature is increased. Moreover, the relaxation peaks on frequency of the imaginary (*Z''*) part moves to a high-frequency region with increasing temperature for all crystal samples.

The loss peak frequency $\boldsymbol{\omega}_{p1}$ can be obtained by fitting the imaginary impedance data and by the variation of relaxation times, Figure 2(b), $\tau_1 = 1/\boldsymbol{\omega}_{p1}$ as a function of reciprocal temperature. The Arrhenius equation $\tau_1 = \tau_0 \exp(\phi/k_B T)$ (where τ_0 is the natural relaxation time and ϕ is the activation energy) permits the determination of the activation energies ϕ (Table 1) of the electrical dipoles in the bulk conductivity at different temperature ranges for the crystals. Continuum current conductivity G_1 (*dc*) can be obtained by using the fit method of the Z' curves at low temperatures. Hence, the linearity between $\ln(G_1)$ and 1/T obtained from Arrhenius relationship $G_1 = \exp(E_{G1}/k_B T)$ (where E_{G1} is the activation energy in the bulk to the *dc* conductivity and k_B is the Boltzmann constant), Figure 2(a), gives the distinct activation energies, E_{G1}, (Table 1) in different regions.

Table 1 presents the activation energies of the crystals. Different values of τ_1 and G_1 are due to the temperature variation rate ranges (Figure 2) for each crystal. As a result, distinct values of the activation energies in regards to the relaxation time ϕ and conductivity G_1 (*dc*) were obtained.

Different electrical conduction mechanisms are involved in the conductivity of the crystals, for instance, proton jumps in hydrogen bonds and heavier ions migration (K^+ and NH_4^+) at higher temperatures, as well as, the rotation and reorientation of ammonium groups in the crystal lattice. In the mixed crystals, the migration of heavier ions and the presence of the lattice defects, as micro cracks, led to the increase in the activation energy values mainly in higher temperature

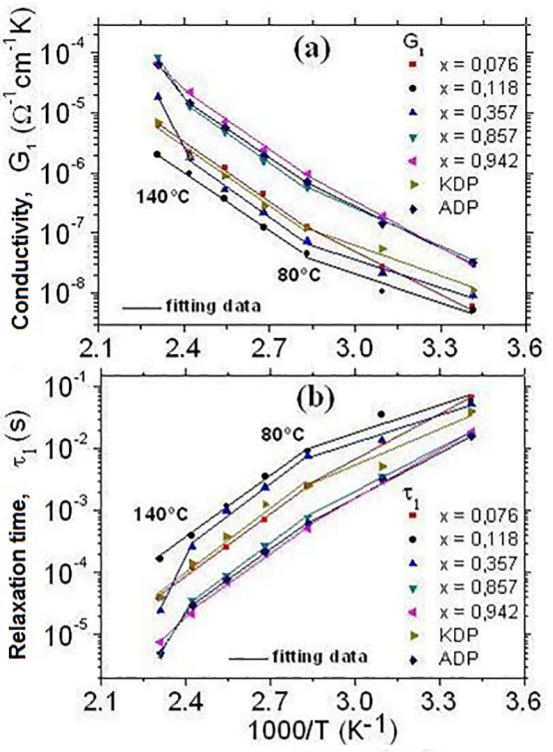

Figure 2: (a) *dc* conductivity G_1 as a function of temperature and (b) variation of relaxation times, $\tau_1 = 1/\omega_{p1}$, as a function of temperature for the crystals.

ranges (Table 1). Hence, the crystals with amount $x = 0.118$ and 0.357 presented lower conductivities at a temperature range of 50 ºC - 140 ºC than those for other crystals, due to the barriers (as micro cracks and inclusion, for instance), which hinder the charge carrier mobility in the crystal lattice.

$KADP_x$ crystals with $x = 0.942$ and 0.857, as well as, ADP present greater conductivity than that on other crystals. This can be attributed to the relative facility of the charge carrier mobility in the ADP and ADP-rich crystals, owing to weaker HN-O bonds when compared to those K-O in the KDP-rich crystals and KDP, which presented lower conductivity. The mixed crystals with $x > 0.8$ and $x < 0.2$ have good quality and, consequently, better conductivity. On the other hand, the mixed crystal with $x = 0.357$ have a relatively low conductivity (Figure 2) due to the micro cracks and inclusions occurrence, contributing to its low quality. The higher values of activation energies between 140 and 160 ºC (Table 1) can be related to heavier ions migration and rotation of atomic groups, hindering the charge carrier mobility.

Other dielectric parameters, as the complex permittivity (ε^*) and complex conductivity (σ^*), have been obtained through the following equations:

$$\varepsilon^*(\omega) = \varepsilon'(\omega) - i\varepsilon''(\omega) = 1/[i\omega C_0 Z^*(\omega)] \quad (2)$$

$$\sigma^*(\omega) = \sigma'(\omega) - i\sigma''(\omega) = i\omega\varepsilon_0\varepsilon^*(\omega) \quad (3)$$

Table 1: Activation energies for the $K_{1-x}(NH_4)_xH_2PO_4$ crystals.

X	Temperature range (ºC)	Activation energy (eV)
0	160 - 80	$\phi_I = 0{,}66$, $E_{G1,I} = 0{,}66$
	80 - 20	$\phi_{II} = 0{,}41$, $E_{G1,II} = 0{,}36$
0.076	160 - 80	$\phi_I = 0{,}67$, $E_{G1,I} = 0{,}64$
	80 - 20	$\phi_{II} = 0{,}49$, $E_{G1,II} = 0{,}29$
0.118	160 - 80	$\phi_I = 0{,}67$, $E_{G1,I} = 0{,}66$
	80 - 20	$\phi_{II} = 0{,}27$, $E_{G1,II} = 0{,}48$
0.357	160 - 140	$\phi_I = 1{,}80$, $E_{G1,I} = 1{,}77$
	140 - 80	$\phi_{II} = 0{,}69$, $E_{G1,II} = 0{,}66$
	80 - 20	$\phi_{III} = 0{,}23$, $E_{G1,III} = 0{,}30$
0.857	160 - 140	$\phi_I = 1{,}53$, $E_{G1,I} = 1{,}44$
	140 - 80	$\phi_{II} = 0{,}65$, $E_{G1,II} = 0{,}66$
	80 - 20	$\phi_{III} = 0{,}45$, $E_{G1,III} = 0{,}44$
0.942	160 - 140	$\phi_I = 0{,}82$, $E_{G1,I} = 0{,}84$
	140 - 80	$\phi_{II} = 0{,}66$, $E_{G1,II} = 0{,}66$
	80 - 20	$\phi_{III} = 0{,}53$, $E_{G1,III} = 0{,}51$
1.0	160 - 140	$\phi_I = 1{,}35$, $E_{G1,I} = 1{,}15$
	140 - 80	$\phi_{II} = 0{,}64$, $E_{G1,II} = 0{,}63$
	80 - 20	$\phi_{III} = 0{,}48$, $E_{G1,III} = 0{,}43$

where ω is the frequency, C_0 and ε_0 are the capacitance and permittivity in the crystal bulk, respectively. These different terminologies on the dielectric analysis are useful, as the crystal dielectric properties are easily extracted by using these specific representations.

Figure 3 shows the real part (σ') and imaginary part (σ'') variations of the conductivity *ac* as a function of the frequency by using a double logarithmic scale for the temperature region of 20 - 160 ºC for the crystals KDP, ADP, and $K_{1-x}(NH_4)_xH_2PO_4$ where $x = 0.076$, 0.118, 0.357, 0.857 e 0.942. Low dependency on the frequency in part of the σ' can be observed at low frequencies and an increased conductivity part as the frequency increased at high frequencies for all crystals. At low frequency regime, the *ac* conductivity in the crystals depends on the temperature.

The conductivity and frequency dependence decreases as the temperature is increased. The σ'' variation as a function of frequency is linear for all crystals, as can be seen in Figure 3. Nevertheless, it changes the inclination, passing through a minimum value at different temperatures for each crystal. The linearity deviation indicated that the ionic contribution increased as the temperature increased in the volume of the crystals, despite their possibility on ionic conduction at low and high frequencies.

The σ' values on the $x = 0.076$ $KADP_x$ crystal increase from 5.5×10^{-9} Ω^{-1} cm^{-1} at 20 ºC to 8.0×10^{-6} Ω^{-1} cm^{-1} at 160 ºC at low frequencies. For $x = 0.118$, the σ' values increase from 5.5×10^{-9} Ω^{-1} cm^{-1} at 20 ºC to 2.0×10^{-6} Ω^{-1} cm^{-1} at 160 ºC. In other words, the larger linearity deviation in σ'', Figure 3, indicates that the $x = 0.076$ sample conductivity is higher than that in $x = 0.118$. Accordingly, the *dc* conductivity in the $x = 0.076$ specimen showed the same behavior, Figure 2(a). Conductive behavior in the σ' and σ'' with some anomalies at different temperatures and frequencies for the $x = 0.357$ sample can be seen in the Figure 3, suggesting the occurrence of lattice distortions, cracks, and other defects, hindering charge mobility. Figure 3 also shows that the electrical resistance decreases as the temperature is increased, contributing to the mobility of heavier ions (NH_4^+, K^+), and suggesting the H_2O molecules diffusion from inclusions to the crystal lattice.

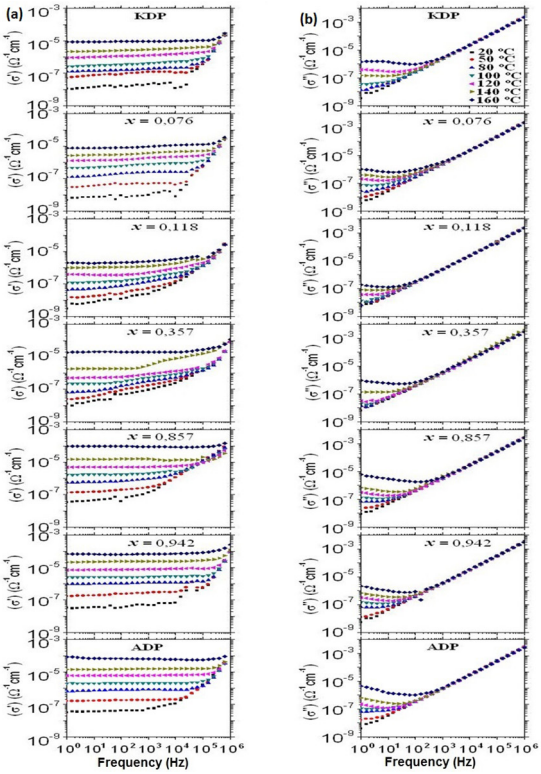

Figure 3: Real part (σ') and imaginary part (σ'') variations of the conductivity ac as a function of frequency and temperature for the crystals.

Figure 4 shows the real part (ε') and imaginary part (ε'') variations of the permittivity *ac* as a function of the frequency by using a double logarithmic scale for the temperature region of 20 - 160 ºC for the crystals KDP, ADP, and $K_{1-x}(NH_4)_xH_2PO_4$ where $x = 0.076$, 0.118, 0.357, 0.857 e 0.942.

Figure 4 shows that ε' values quickly increase at low frequencies and at high temperatures, owing to the ion mobility effect in the crystal frame and increased polarization of the electrodes. Furthermore, ε'' can be formulated as a two sum of electrical behaviors, which are related to the conduction of the long-range mobile ions and the reorientation of dipoles (as group of atoms in lattice) in the mixed crystals under an external electrical field. These two behaviors are, respectively, regarding to the 1/ω variation at low-frequency and broad incomplete bands at high-frequency (Figure 4). As indicated in Figure 4, crystals become conductors when the temperature is increased as already observed. Graphic comparison in Figure 4 shows that the ε' values in the $x = 0.076$ sample are greater than those in the $x = 0.118$

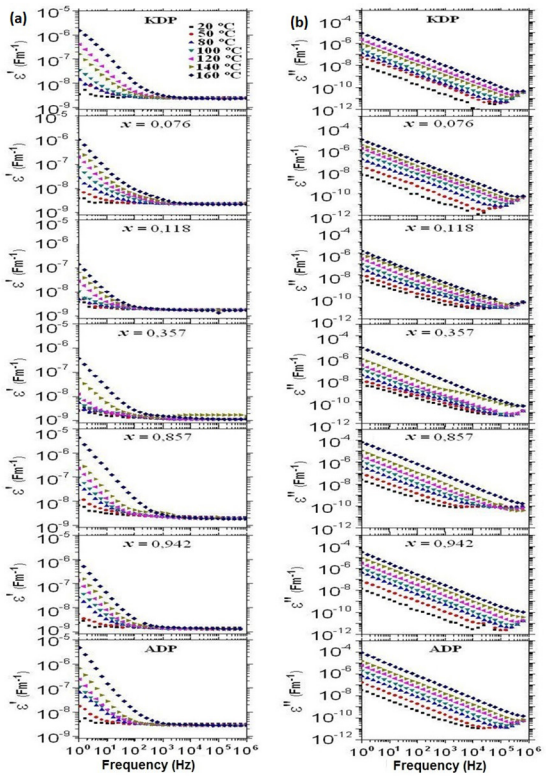

Figure 4: Real part (ε') and imaginary part (ε'') variations of the permittivity ac as a function of frequency and temperature for the crystals.

sample at low frequencies and at high temperatures, owing to the x = 0.076 crystal good quality, contributing to the ionic mobility increase. Furthermore, the incomplete bands in ε'' for the x = 0.118 crystal, Figure 4, are broader than those showed in ε'' for the x = 0.076, that is, the dipolar relaxation contribution is more expressive in the x = 0.118 sample than that in the x = 0.076 sample mainly in low temperatures. Figure 4 also shows that both ε' and ε'' curves for the x = 0.357 crystal have anomalies which indicate the anomalous structural behavior in regards to the lattice defects. Therefore, $KADP_x$ crystals with higher quality, x = 0.942 and 0.076, have better conductivity compared to other mixed crystals. On the other hand, occurrence of distortions and other defects in the crystal lattice are detrimental to the increase of ammonium or/and potassium content x in the mixed crystals. This result indicates that the conductivity is degraded in the crystal with intermediate x content. In the mixed crystals the microscopic environment around ammonium, close to the intrinsic structural form of the ion ammonium in the ADP-pure, has higher conductivity than that in the microscopic environment around potassium in the mixed crystal with more similarity to the KDP intrinsic structural form.

In summary, ADP-pure and ADP-rich crystals with bigger microscopic environment around ammonium than that around potassium have microstructural behavior with easier charge carrier mobility than that for KDP and KDP-rich crystals. This contributes to the higher electrical conductivity in environment around ammonium than that in environment around potassium with strongest bonds, K-O. Moreover, the occurrence of the lattice defects as micro cracks and inclusions (mainly in intermediate amounts x), leading to the crystal quality degradation, hinder even more the charge carrier mobility. Accordingly, electrical conductivity by the charge carriers is strong influenced by crystal frame aspects. Moreover, the chemical bond strengths in the K^+, NH_4^+, and $H_2PO_4^-$ ions and the organization form between ions to compose the crystal during the crystal growth and the differences of the ionic radius (K^+ and NH_4^+) have important role in the conductivity and defect occurrence in mixed crystals.

4. Conclusion

Electrical conductivities of the pure crystals KDP and ADP, as well as, $KADP_x$ (x = 0.076, 0.118, 0.357, 0.857, 0.942) mixed crystals were investigated by means of Impedance Spectroscopy under the influence of increase in frequency and temperature. They were grown by solvent evaporation method. Zview simulation software was used to theoretically fit conductivity results. These crystals are dielectric-type crystals at room temperature and become ionic conductors when the temperature is increased. This conduction behavior follows the Arrhenius equation with which the different activation energies were determined. Proton jumps in hydrogen bonds, heavier ions migration (K^+ and NH_4^+), and rotation and reorientation of ammonium groups act as charge carriers, contributing to electrical conduction. For ADP-rich ($x > 0.8$) and pure ADP crystals the conductivities are higher than those for KDP-rich ($x < 0.2$) and pure KDP, owing to the easier charge carrier mobility in the microscopic environment around ammonium than that in the microscopic environment around potassium. Results suggested that the $KADP_x$ (x = 0.94) crystal at 80 - 140 ºC temperature range is the best conductor. Lattice defects may reduce electrical conductivities in the crystals with intermediate x composition. Complex permittivity and complex conductivity *ac* were also obtained for these crystals.

5. Acknowledgment

The author is grateful to CAPES (Brazil) for the financial support of this work, and also thank Bianchi R. F. and Franco C. J. for their very much appreciated inputs.

6. References

1. Barret JJ, Weber A. Temperature dependence of optical harmonic generation in KDP and ADP crystals. *Physical Review*. 1963;131(4):1469-1472.

2. Glass AM, Lines ME. *Principles and Applications of Ferroelectric and Related Materials*. Oxford: Oxford University Press; 1977. p. 293-321.

3. Boukhris A, Souhassou M, Lecomte C, Wyncke B, Thalal A. Evolution of the structural and mean square displacement parameters in $(NH_4)_xK_{1-x}H_2PO_4$ solid solutions versus concentration and temperature. *Journal of Physics: Condensed Matter*. 1998;10(7):1621-1641.

4. Zaitzeva N, Carman L. Rapid Growth of KDP-type Crystals. *Progress in Crystal Growth and Characterization of Materials*. 2001;43(1):1-118.

5. Ren X, Xu D, Xue D. Crystal growth of KDP, ADP, and KADP. *Journal of Crystal Growth*. 2008;310(7-9):2005-2009.

6. Souza FM. *Preparação e caracterização estrutural e elétrica de cristais mistos de* $K_{1-x}(NH_4)_xH_2PO_4$. [Dissertation]. Ouro Preto: Rede Temática em Engenharia de Materiais - Universidade Federal de Ouro Preto; 2009. 76 p.

7. Xu D, Xue D. Chemical bond simulation of KADP single-crystal growth. *Journal of Crystal Growth*. 2008;310(7-9):1385-1390.

8. Chen RH, Yen CC, Shern CS. Studies of high-temperature phase transition, electrical conductivity, and dielectric relaxation in $(NH_4)H_2PO_4$ single crystal. *Journal of Applied Physics*. 2005;98(4):044104.

9. Chen RH, Yen CC, Shern CS, Fukami T. Impedance spectroscopy and dielectric analysis in KH_2PO_4 single crystal. *Solid State Ionics*. 2006;177(33-34):2857-2864.

10. Jonscher AK. Dielectric relaxation in solids. *Journal of Physics D: Applied Physics*. 1999;32(14):R57-R70.

11. Cole KS, Cole RH. Dispersion and Absorption in Dielectrics. 1. Alternating Current Characteristics. *Journal of Chemical Physics*. 1941;9(4):341-351.

12. Subhadra VK, Syamaprasad U, Vallabhan CPG. High-temperature phase transitions in pure and deuterated ammonium dihydrogen phosphate: Conductivity and dielectric measurements. *Journal of Applied Physics*. 1983;54(5):2593-2596.

13. Harris LB, Vella GJ. Direct current conduction in ammonium and potassium dihydrogen phosphate. *The Journal of Chemical Physics*. 1973;58(10):4550-4557.-